INCLUSION OF INTER CRYSTAL SCATTER DATA IN PET

J.E. Gillam[1]*, P. Solevi*[1]*, J.F. Oliver*[1] *and M. Rafecas*[1,2]

[1]Instituto de Física Corpuscular, CSIC–Universitat de València
[2]Departament de Física Atómica, Molecular i Nuclear, Universitat de València.

ABSTRACT

In PET, as the spatial resolution of the measurement system is increased, multiple interactions of a single photon may be separately measured and such events are often removed from the data used in image reconstruction. While for some PET imaging tasks this effect is unimportant, for primate, brain and high-spatial-resolution imaging where sensitivity is important, such Inter Crystal Scattering (ICS) events may constitute a large fraction of the measured data. On-the-fly list-mode image reconstruction is generally required in order to use all the information provided by ICS. Simulated One-Pass List-mode image reconstruction is used in this investigation to study the inclusion of ICS information into the reconstructed image using data acquired with the AX-PET prototype. In almost all cases an increase in image quality was observed, particularly for larger features. A small resolution penalty was also observed.

***Index Terms*—** Positron Emission Tomography, Inter Crystal Scatter, List-mode, Image Reconstruction

1. INTRODUCTION

In Positron Emission Tomography (PET) coincident measurement of two 511 keV photons are used to define a Line of Response (LoR), taken to represent the collinear trajectory of photons produced in positron annihilation. However, photons not undergoing photoelectric absorption either result in non-photo-peak energy deposition or multiple coincidence and are often removed from measured data. When Low-Energy Thresholds (LETs) are high and only standard coincidence is accepted, detection-space modeling can indirectly redress some of the effects of ICS [1]. However, this indirect approach sacrifices sensitivity due to the high LET. Reduction in the LET can enhance sensitivity but may lead to the direct measurement of Compton ICS as multiple-coincidence events (shown in Fig 1) that then must be addressed in the process of image reconstruction.

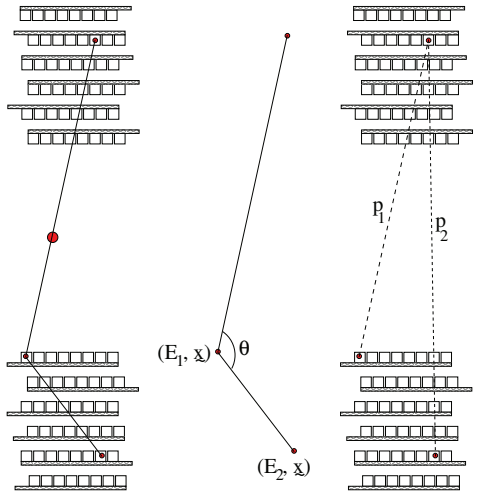


Fig. 1. Inter Crystal Scattering. One annihilation photon Compton scatters before photoelectric absorption. Each sequence is associated with a scattering angle. An ICS LoR pair is defined, each with an associated probability determined via Compton kinematics and the Klein Nishina cross-section.

At 511 keV for most scintillators used in PET, Compton scattering has a higher interaction cross-section than photoelectric absorption. However, for a large range of Compton scattered photons, photoelectric absorption is the dominant process and attenuation lengths can be small in comparison to measurement resolution (between ≈1.3–13 mm in LYSO). Should the second interaction be spatially separable from the first (by a pixel boundary or other means) ICS will be measured. While the proportion of ICS measurement in any given data set will be affected by the material, it is also governed by the spatial resolution. As detection resolution increases, so too will the preponderance of ICS measurements. For PET using LYSO this becomes important at a resolution of 1–2 mm (the attenuation length of a low energy Compton scattered 511 keV photon in LYSO).

In single photon imaging the application of Compton kinematics can provide the ability to reduce the incident trajectory of single photons to the surface of a cone. Compton imaging requires the measurement of multiple interactions of a single photon and should scintillator detectors be em-

J.G. is supported by the Spanish Ministry of Science and Innovation through "Juan de la Cierva" contract. P.S. was supported by Marie Curie IEF grant 237620 for the project INSPET. JFO was supported by the JAE-Doc modality of the program Junta para la Ampliacin de Estudios. The work is supported by The Ministry of Science and Innovation FPA2010-14891. The authors are indebted to the AX-PET collaboration for acquiring all data analyzed.

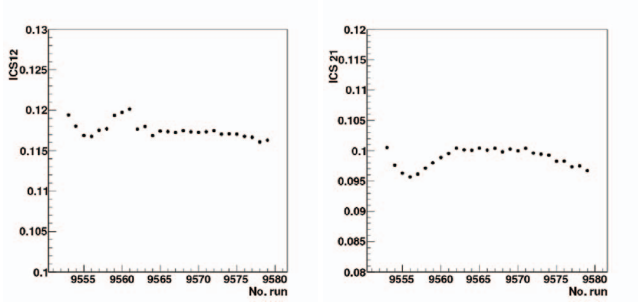


Fig. 2. Fraction of ICS events (compared to Golden) measured in each AX-PET module as a function of the run number for the data used in image reconstruction.

ployed, such measurements would qualify as ICS. However, scintillation-based PET measurement does not generally provide sufficient resolution (or interaction separation) such that Compton camera imaging is directly useful. Instead, Compton kinematic processing has been proposed to differentiate between the two possible LoRs in an ICS pair [2]. Often the success of identification is less than optimal so that increasing measurement statistics is often preferred to ICS inclusion. Here, the use of both LoR possibilities during image reconstruction is proposed and tested as an alternative.

In this investigation, experimental ICS information from a novel prototype detection system, the AX-PET [3], is used in combination with Simulated One Pass List-mode (SOPL) [4, 5] - based on list-mode Maximum-Likelihood Expectation-Maximization (MLEM) [6] image reconstruction algorithm - to assess the utility of inclusion of ICS information into the reconstructed image. Only standard (double) and triple coincidence are considered and different methods of including ICS data into the useful data set are addressed.

2. MATERIALS AND METHODS

For all data acquisition, the NEMA-NU4 IQ (mouse) phantom was used [7]. However, instead of two cold regions one of the voids was filled with activity of concentration of approximately three times that of the uniform region of the phantom. During analysis, measurement of the Recovery Coefficient (RC) and standard deviation of the RC (STD-RC) were made in accordance with the NEMA protocol [7] for each of the rod-features in the phantom.

2.1. The AX-PET Prototype

The AX-PET prototype is a recently developed dual-head PET detector for which each head provides high resolution three dimensional measurement [3]. Each AX-PET detector is composed of six detection layers. Each detection layer is composed of an array of eight axially oriented LYSO crystals ($3\times3\times100$ mm^3) that are optically coupled to a second orthogonal array of Wave-Length Shifting (WLS) strips, both are read out by Geiger-mode Avalanche Photo Diodes (G-APDs). The resultant measurements are trans-axially discretized with 3×3 mm^2 resolution (including Depth of Interaction) and continuous measurement ($\approx$ 1.5 mm FWHM) in the axial dimension. All measurements were subject to hardware thresholds that limited recorded data to only those events for which the total energy recorded in each detector head was in the 511 keV photo-peak. The resultant data set had approximately 20% ICS interactions (shown in Fig 2). ICS interactions consisted of single-interaction measurement in one of the AX-PET heads and measurement of two interactions in the other. Because of possible single-layer degeneracy, the two interactions were only deemed acceptable if they occurred in different layers (depth-wise) of the AX-PET detector stack.

2.2. Inter-Crystal Scattering

Triple ICS measurement, as shown in Fig 1, results in two possible LoRs. Each is defined by a unique interaction in one module and two interactions that compose an ICS pair in the other. In order to include ICS information into the data for image reconstruction either both ICS end-points must be used or one must be selected as the first interaction.

One approach used to determine the primary interaction for an ICS sequence is based on the Klein-Nishina (KN) differential cross-section:

$$\begin{aligned}\frac{d\sigma}{d\Omega} &= \frac{Zr_0^2}{2}([1+\gamma(1-\cos\theta)]^{-3} - \\ &\quad \sin\theta^2[1+\gamma(1-\cos\theta)]^{-2} + \\ &\quad [1+\gamma(1-\cos\theta)]^{-1}) \end{aligned} \quad (1)$$

where $\gamma = E_0/m_e$ and E_0 is the energy of the incident photon. In Eq. 1 $\cos\theta$ can be computed for each ICS interaction using either the geometrical angle (θ_G), given by the angle at the interaction (Fig 1 center) or determined using the energy deposited at the interaction site (θ_E, determined via Compton kinematics). In either case the result is that each ICS interaction can be associated with a KN cross-section should it be the primary interaction. This value can then be used in two ways. Either it can be used to discriminate between the two LoR possibilities (the LoR with the smallest value is removed from the data set), or it can be used to weight (after normalization) each LoR in a combined back-projection/projection calculation (essentially using a weighted V-shape).

The optimal scattering angle for use in weighting or discrimination is guided by the scanner spatial and energy resolutions. AX-PET is characterized by good energy resolution (FWHM=11.8% at 511 keV) and a spatial resolution that ranges from 2.03 mm FWHM in the trans-axial dimensions to 1.75 mm in the axial coordinate. In the following study the KN probabilities were computed by means of a pure geometrical approach since the spatial resolution was considered superior. The KN-weighting was calculated for each ICS event

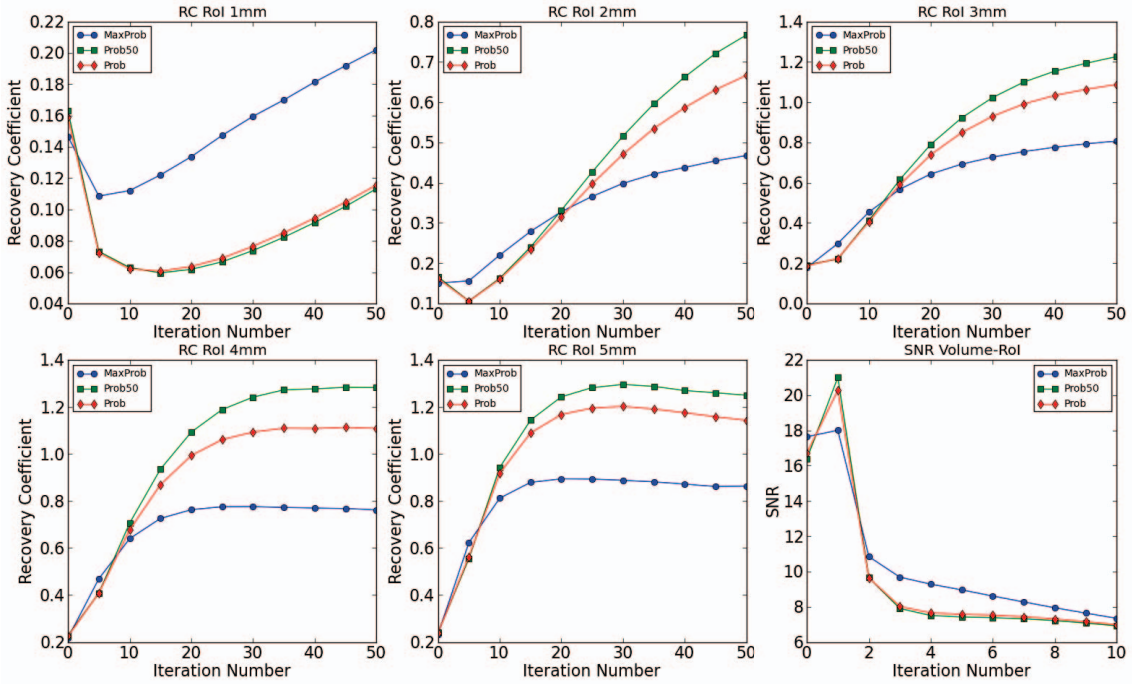


Fig. 3. The Recovery Coefficient for all rod-features and the Signal to Noise Ratio (SNR) in the uniform region of the NEMA phantom reconstructed using only ICS events. Results are shown for discrimination (MaxProb), even weighting (Prob50) and weights based on the KN cross section (Prob).

in the data and the results organized into seven data sets for subsequent image reconstruction: Golden (no ICS), ICS only using discrimination (MaxProb), equal-weighting (0.5 each - Prob50), Klein-Nishina weighting (Prob) and combined data (Golden + ICS) for each ICS treatment. The investigation was then categorized into two independent studies; those containing only ICS events and combination data (Golden and ICS).

2.3. Image Reconstruction

SOPL is a method of image reconstruction that provides on-the-fly calculation of the system matrix elements and is intended for List-mode MLEM. SOPL is based on calculation of line-intersections using the Siddon algorithm [8] for computational simplicity. Random sampling from models of detection uncertainty provides a subset of possible Siddon rays (different at each iteration) for subsequent computation. SOPL provides a hybrid approach to system matrix calculation which combines properties of both Monte-Carlo and analytic methods to calculate matrix elements [4, 5]. While SOPL does not guarantee convergence, it does provide an on-the-fly list-mode approach for which no data ordering or pre-sorting is required and so is a natural candidate to address inclusion of unusual data types such as ICS. In this investigation the uncertainty models used for SOPL were taken as 2.5 mm uniform distributions oriented with and centered at each crystal in the trans-axial plane and a normal distribution of 0.5 mm standard deviation in the axial (continuous) dimension [4]. For all studies five Siddon-rays were used for each LoR and a small (0.5 mm standard deviation) image-space model was employed. For reconstruction using both LoRs represented by the ICS-pair each possible LoR was sampled using the same number of Siddon-rays, with corresponding weights to compose a V-shaped back-projection/projection.

3. RESULTS AND ANALYSIS

Images reconstructed using only data containing ICS events and an evenly weighted V-shape produced optimal RC values for all but the smallest rod feature of the NEMA phantom (shown in Fig 3). While weighting using the KN provided improved recovery compared to discrimination, weighting each ICS LoR by 0.5 was optimal. For the smallest (1 mm) rod, discrimination proved superior, indicating a small resolution degradation occurs when using both ICS LoRs during image reconstruction. The uncertainty in the RC showed a similar relationship, (shown for two sample features in Fig. 4).

The results were similar upon inclusion of Golden events only for the smallest (1 mm) feature. For all other rod-features, discrimination proved to have superior noise properties to weighting. The uncertainty in the RC values are shown in Fig. 5 for two representative (1 and 3 mm) features. In Fig. 5 results are also given for images reconstructed using a pre-calculated system matrix, yet cautious comparison is required due to differing system models and experimental considerations. For SOPL, it was observed that while Golden

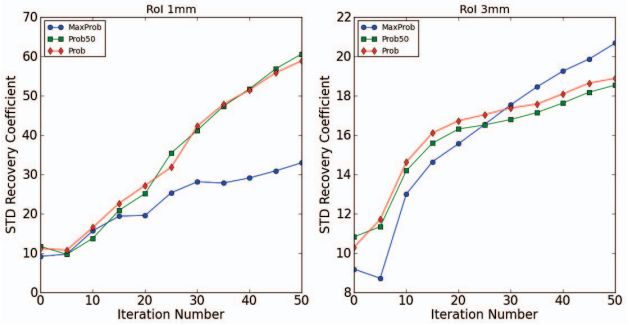


Fig. 4. Standard deviation of the RC for two representative rod-features of the NEMA phantom. Only ICS event were used in reconstruction.

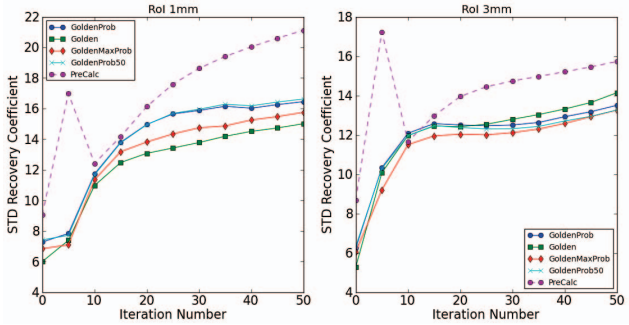


Fig. 5. Standard deviation of the RC for two representative rod-features of the NEMA phantom. Golden (results from a pre-calculated system matrix are included for comparison) and golden plus ICS events using MaxProb, Prob50 and Prob analysis are shown.

events alone produced the most accurate RC values for the smallest feature, with a smaller STD-RC than with inclusion of any ICS information, this was not the case for all other feature sizes. For larger features, discrimination was optimal and ICS event exclusion was worst - particularly at later iterations. Evenly weighted V-projections were only slightly better than those with KN-based weights.

4. DISCUSSION AND CONCLUSION

The results indicate that in the absence of more accurate information using both ICS LoR possibilities (weighting) in the process of image reconstruction provided increased accuracy compared to the discrimination method. However, a small degradation in the spatial resolution was observed. Unexpectedly, unweighted (or evenly weighted) V-projections proved here to be superior. While it is thought that the observed difference was due to the weighting parameter selected (the geometrically determined KN) other factors may also contribute to the quality of the reconstructed image.

Parameters affecting image quality and resolution fall into two broad categories: data-based and model based. Model based effects include the choice of θ_G or θ_E (or a combination of the two), the use of the KN(θ) in determining weights and the inclusion of extra information such as the photoelectric cross-section of the scattered photon. Data-based effects include data statistics, interaction separation, measurement geometry and differences in algorithmic convergence.

Data statistics were of specific importance in optimal treatment of ICS information. When Golden events were included into the reconstructed data set, the best treatment of ICS information was seen to change. The role of data statistics in the inclusion of ICS measurement is directly relevant to high-sensitivity high-resolution PET studies, where many measurements may be lost to ICS should they not be included into the useful data. Also of particular interest is the type of ICS events included into the data. The angle between ICS LoRs (p_1 and p_2 in Fig 1), governed by recoil photon trajectory, determines whether the ICS-triple forms a V-shape or, instead, simply a thick wedge-shaped geometry. Such thick lines may be responsible for the observed resolution degradation. Some ICS measurements may be less worth preserving than others and the relative utility of different ICS measurements may be of importance. This investigation presents an approach to ICS inclusion and preliminary analysis. However, extended investigations are required in order to fully understand each of these effects.

This investigation addressed the inclusion of ICS information during image reconstruction. It was shown that in almost all cases inclusion of ICS improved image quality, at a small expense to resolution. However, the optimal method of inclusion of ICS information was shown to be dependent on the data statistics. When a large number of standard data was available (including Golden events), then discrimination was optimal. However, when few data were available (ICS only) then reconstruction using both ICS LoRs was shown to be superior. While weighting was of utility, it was shown that the choice of weighting parameter was important and should a poor choice be made, image degradation was observed in comparison to using an unweighted ICS LoR pair.

5. REFERENCES

[1] J. Qi et al., Phys. Med. Biol, vol 43 (1998) 1001

[2] M. Rafecas et al., Phys. Med. Biol, vol 48 (2003) 821-848

[3] P. Beltrame et al., Nucl. Inst. & Meth. A., vol. 654 no 1 (2011) 546-559

[4] J. Gillam et al., Fully 3D Conf. Proc. (2011) 310-13.

[5] J. Gillam et al., NSS-MIC Conf. Proc. (2011) 4206-10.

[6] A.J. Reader, Int. Journ. of Imag. Sys. & Tech. vol. 14 no. 3 (2004) 139-45

[7] NEMA 2008 NEMA Standards Publication NU 4 - 2008

[8] R.L. Siddon, Med. Phys. vol. 12 no. 2 (1985) 252-255